Depth Sensing by Variable Baseline Triangulation

J. Clark and A. M. Wallace
Dept of Computing and Electrical Engineering
Heriot-Watt University
Riccarton, Edinburgh, EH14 4AS, United Kingdom
jclark@cee.hw.ac.uk and andy@cee.hw.ac.uk

Abstract

The design and development of a variable baseline triangulation system is described. The sensor employs planar elliptical mirrors in a novel design to allow dynamic reconfiguration of the triangulation geometry. This permits the acquisition of depth maps of a scene with varying levels of occlusion and depth resolution; combining these images allows a more complete scene description of complex objects. The operation of the sensor is illustrated by experimental data.

1 Introduction

Depth ranging using laser triangulation is a mature and popular technology for gauging, profiling and 3D surface mapping [3] [4] [8]. A common problem found with conventional triangulation systems is that of occlusion which occurs when the viewing system cannot observe the projected laser light, with no depth data being gathered in the occluded area [4] [2]. Typically the separation of the laser projection system and the viewing camera (baseline separation) determines both the level of occlusion and the accuracy of the depth data. The designer of the triangulation system has to balance occlusion with accuracy when deciding upon the geometry of the system. Large areas of occlusion within a depth image can have adverse affects on subsequent processes such as segmentation and model based recognition and location.

A common solution to the occlusion problem is to increase the number of cameras viewing the scene [1] [4] [5]. This can minimize occlusion to an extent, but is still highly dependent upon the object being mapped, and each camera has to be carefully calibrated to produce consistent results.

This paper describes a triangulation sensor that can vary its geometry to produce multiple range maps of a scene with varying levels of resolution and occlusion. The sensor employs planar elliptical mirrors that allow the user to dynamically reconfigure the sensor, without the need for re-calibration. Depending upon the camera position, the user can specify a laser projection geometry which is co-linear to the camera optical axis or separated by any angle up to approximately 45 °.

BMVC 1995 doi:10.5244/C.9.23

2 Optional designs for variable baseline geometry

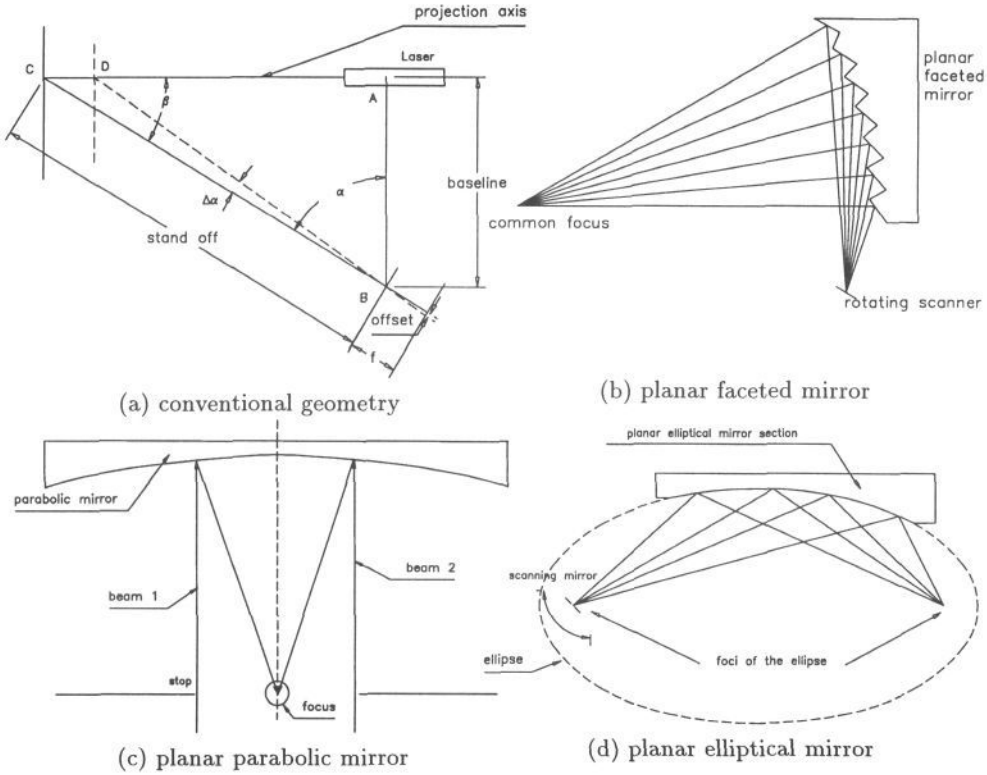

Figure 1: Triangulation using a (a) conventional triangulation geometry; variable baseline triangulation using (b) a planar faceted mirror; (c) planar parabolic mirror; (d) planar elliptical mirror.

Figure 1(a) demonstrates a conventional fixed triangulation geometry, where A and B are nodal points representing the optical axis of a camera lens (B) and projective axis of a laser beam (A) respectively. The line BC represents the optical axis of the camera, with AC representing the projection axis of a laser beam. The baseline separation (AB) is the shortest distance between the optical centre of the camera and the projection axis of the laser beam. The stand-off distance is defined as the distance from the intersection of the projection and optical axes (C) to the optical centre (B). Due to a parallax effect, a change in the height of the object, point D, results in a ray of light entering the camera at an angle $\Delta\alpha$ to the camera axis. The angle $\Delta\alpha$ is determined by the observed offset position of the light ray on the sensor plane. The geometry of a conventional system is fixed, the angle β and the baseline separation cannot be dynamically changed, and if occlusion occurs no data is gathered in the occluded area.

Figures 1(b)-(d) show 3 optional designs which allow the angle of the projected laser light (α) to be varied in a controlled manner, with the plane of the laser passing through a common focal point for all α. Calculation of depth depends heavily on an accurate knowledge of the laser plane. The design which we have implemented and describe in this paper utilizes a planar elliptical mirror,and is described in more detail in Section 3.

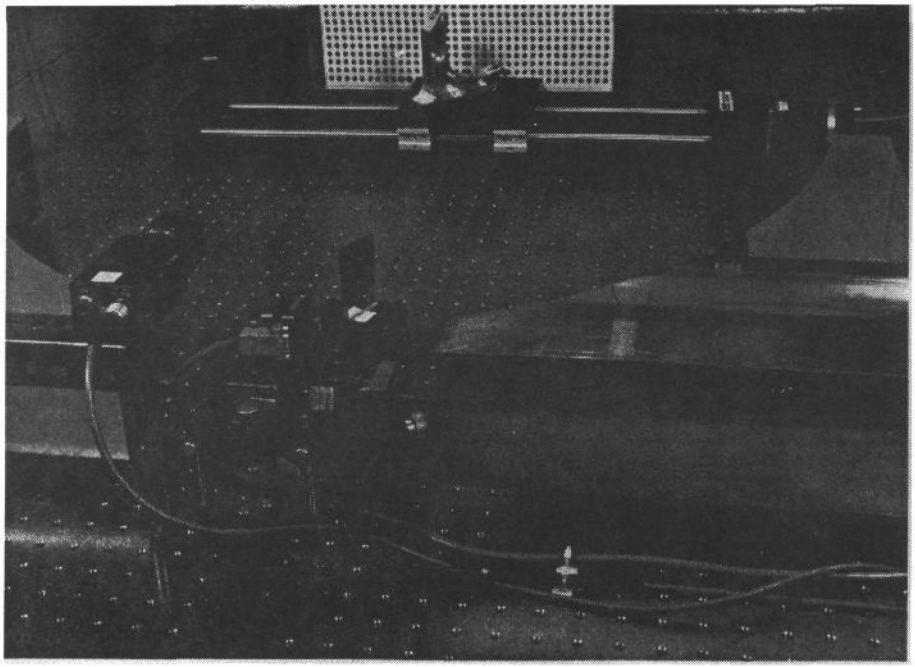

Figure 2: The prototype variable baseline sensor.

3 A variable baseline triangulation system

The variable baseline geometry shown in Figure 4 has a fixed CCD camera (9) but has a laser projection geometry which is variable. This allows the user to acquire multiple depth maps of a scene at different angles of projection to the laser plane, i.e. at variable triangulation geometry. Figure 2 shows the actual prototype system. Depth data acquired with a large angle of illumination has a high resolution but is likely to suffer greatly from occlusion. At a low angle of illumination the data is relatively un-occluded but has lower resolution. Intensity data is acquired from the single, central camera.

The major innovation is the use of a planar elliptical mirror. This has the special property that light projected through one focus towards the mirror will be reflected and focussed at the other focus of the ellipse. The variable baseline sensor employs the optical properties of elliptical mirrors to provide a variable baseline or angle of illumination, i.e. the angle between the major axis of the elliptical mirror and the illuminating laser sheet. A dual mirror arrangement is

used to further minimize occlusion; this allows us to vary the angle of illumination between $5 - 45^\circ$ to the left and right of the major axis.

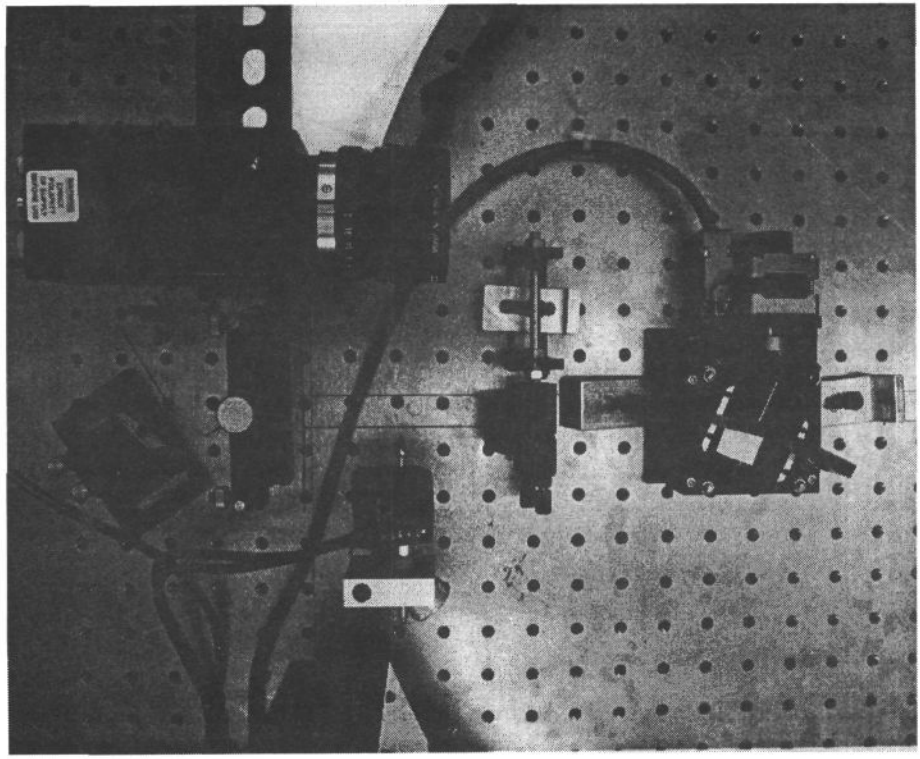

Figure 3: Scanning and projection optics.

Figure reffig:system demonstrates the operation of the variable baseline sensor. A collimated beam of laser light (1) is projected onto a rotating galvanometer scanner (2) to form a line, which is then projected onto a plane mirror (3) placed at the near focus of the pair of elliptical mirrors. From here it is reflected to one of the elliptical mirror sections (4) and hence to the far focus of the ellipse (5), where a translation stage (6) is positioned perpendicular to the major axis of the ellipse. The plane mirror is mounted on a rotating stage (7), whose rotation results in a variation of the angle of illumination. To scan an object (8) the plane mirror is moved to give the maximum illumination angle, the object is then stepped through the beam to acquire a depth image of the scene. Figure 3 shows a close up view of the rotation stage and projection optics. If regions of interest are occluded then the angle of illumination can be reduced and a complimentary depth image can be acquired. This process can be repeated using both the left and right mirrors until occlusion has been minimized within the bounds of the sensor geometry. A PC controls the rotation and translation stages, image capture, determination of occluded areas and calculation of depth.

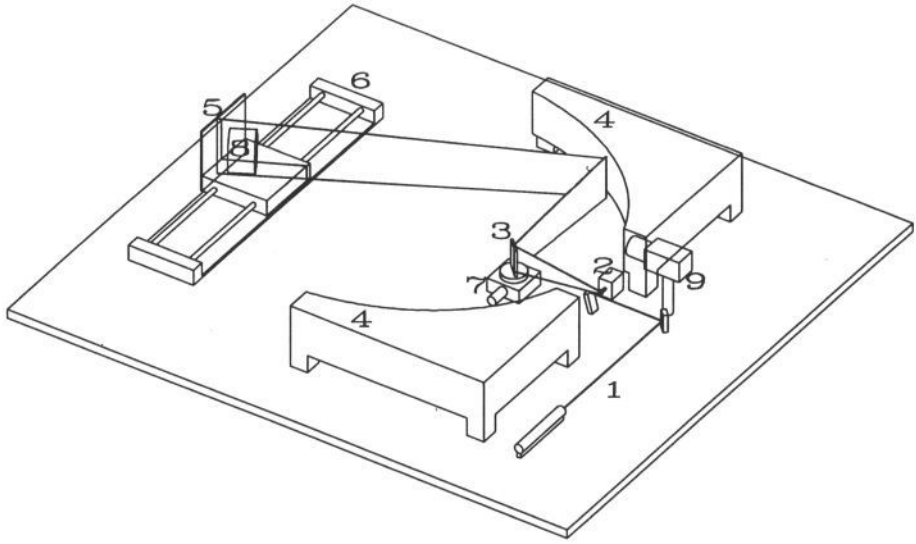

Figure 4: Schematic of variable baseline sensor.

4 Analysis of the system geometry

A representation of the system geometry is demonstrated in Figure 5. The observed light stripe, imaged by the camera lens onto the plane of the CCD at o and creating an angle α with the optical axis relates to a range R (along the laser plane, from baseline to $R+$) calculated from

$$\pm R = \frac{Bp}{b_1} \tag{1}$$

It can be shown that the precision, ΔR, the uncertainty related to a measurement of depth varies with the depth being measured as,

$$\Delta R = \Delta s \frac{-Bf}{(f\cos\gamma + o\sin\gamma)^2} \quad \& \quad \Delta R = \Delta s \frac{-Bf}{(f\cos\gamma - o\sin\gamma)^2} \tag{2}$$

with the former for light rays imaged on the CCD sensor below the optical axis, and the latter above the optical axis. In terms of the measured range R_c (range from the camera to the object surface) this can be expressed as

$$\Delta R = \Delta s \frac{-Bf}{\left[(f\cos\gamma + \left(\frac{d\cos\beta f}{R_c}\right)\sin\gamma)^2\right]} \tag{3}$$

where Δs is the smallest change in position that can be measured by the CCD element placed at the back focal plane of the lens. The value of Δs is in effect the resolution of the camera. This is considered to be a constant value, dependent upon the size of the CCD pixels, angular resolution of the lens, focal length of lens and

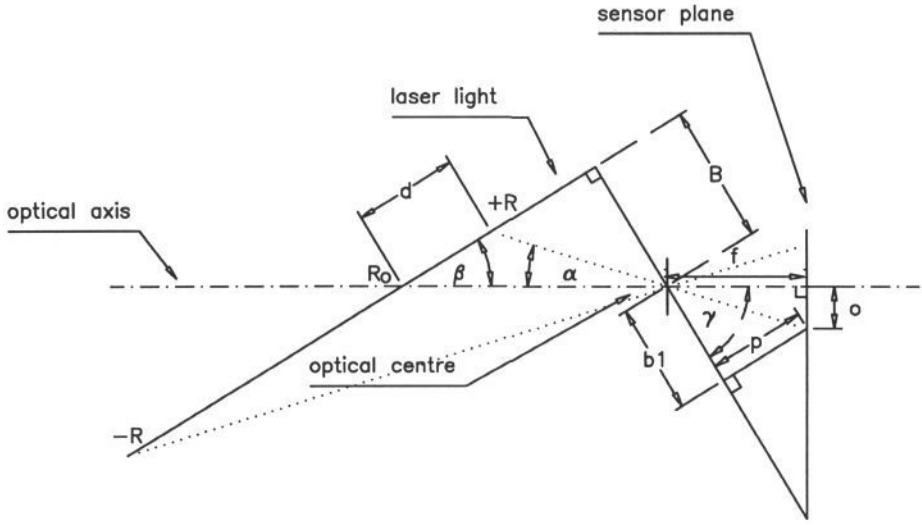

Figure 5: Geometry of variable baseline triangulation system.

degree of sub pixel accuracy [9]. For example the Pulnix TM520 camera used has an approximate pixel size of $8.6\mu m$ (H) by $8.3\mu m$ (V). If we are measuring changes in depth as changes in position horizontally along the CCD then $\Delta s = 8.6\mu m$ if there is no sub pixel precision. If there is a degree of sub pixel precision, n, then $\Delta s = \frac{pixel\ size}{n}$.

Figure 6 demonstrates how the precision ΔR is expected to vary with the measured range and variation of the angle of illumination, β, for the prototype sensor described previously. The stand-off distance has been set to $900mm$, the focal length approximately $25mm$ and the level of sub-pixel accuracy has been assumed to be $\frac{1}{4}$ ($n = 4$). The angle of illumination has been varied between 5° and 45° in 5° steps. In this initial trial of the sensor the base plane (the maximum range from the camera which can be measured, a depth of $0mm$ in the world coordinate system) has been set to coincide with the intersection of the projected laser plane and optical axis, R_o in Figure 5, which has been previously defined as the stand-off distance. The base plane position is decided at setup time; placing it at Ro ensures a high degree of precision but limits the range of depths that can be measured, the balance between precision and range of measureable depths will be decided by the scene which is to be measured.

It can be seen that reducing the baseline to minimize possible occlusion effects, i.e. altering the angle of illumination from 45° towards 5°, will result in poorer precision. However, over short ranges the precision can still be reasonably high.

5 Experimental Results

Figure 7 demonstrates the ability of the sensor to acquire multiple depth images with varying triangulation geometry. Figure 7(a) shows an intensity picture of the object being scanned, in this case a fan assembly. Figures 7(b)-(f) show depth

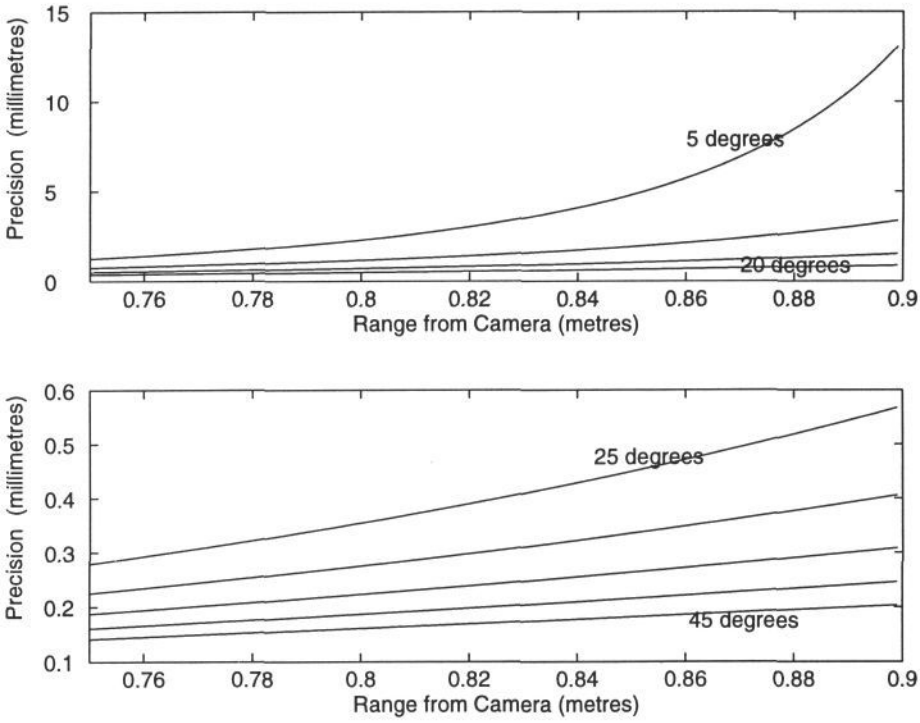

Figure 6: Predicted precision in depth with varying angle of illumination.

images obtained from both the left (L) and right mirrors (R).

All five images display a level of occlusion; the visibility of each surface is indicated in Table 1. A full depth map would incorporate data from each image. For example in this case (b) might provide the main image, with (f) filling in surfaces 2 and 5, and part of surface 3. Image (e) provides the most detailed insight into surface 3. All five images contain useful data relating to the curved surfaces a-e. Wherever possible the high resolution data would be used.

An initial test of system accuracy was conducted by measuring the height of a series of flat planes from a known datum. The average accuracy relating to the height ranges found in Figures 7 (b), (c) and (d) was found to be $\pm 0.334mm$, $\pm 0.51mm$ and $\pm 3.33mm$ respectively. Accuracies in the final sensor are expected to be higher. The data produced by the prototype sensor was without the benefit of an accurate laser plane and camera calibration.

6 Discussion

Triangulation is an effective technology for acquisition of range maps. We have described the design and implementation of a prototype with reconfiguarble ge-

Surface Visibility	Angle Of Illumination				
	Left Mirror			Right Mirror	
	35°	25°	20°	10°	25°
Visible	1, 4	1, 4	1, 4, c-e	3	1-5
Partial	a-e	a-e	a, b, 3	1, 3, 5, d, e	c, d
Occluded	2, 3, 5	2, 3, 5	2, 5	2, a-c	a, b, e

Table 1: Object surface visibility with respect to different laser illuminating angles as shown in Figure 7(a).

ometry to vary the effective baseline separation. This has been demonstrated by the acquisition of range maps at several different angles of illumination to acquire depth data at variable resolution and areas of occlusion.

Development of the sensor continues. Some re-engineering of the system components is necessary to address problems of system integration and calibration revealed at the prototype stage. A full analysis of system performance is required in terms of the accuracy and repeatibility of the range data. We wish to demonstrate further how an optimal depth map can be combined in terms of completeness and accuracy of the sampled data points. We wish also to use the depth data from multiple views to determine inter-reflections within range maps by tracking the inter-reflections through subsequent views. This will allow us to alleviate the effect of inter-reflections on highly specular objects, a common problem with triangulation sensors resulting in the generation of erroneous depth data. The system should also provide registered depth and intensity data. This should produce (a) a richer and more robust scene description for subsequent recognition and location of objects; and (b) detailed image inspection using either mode in isolation as appropriate. Finally, we wish to improve the robustness and flexibility of the system by using the processed intensity and depth data to control the low level acquisition of data.

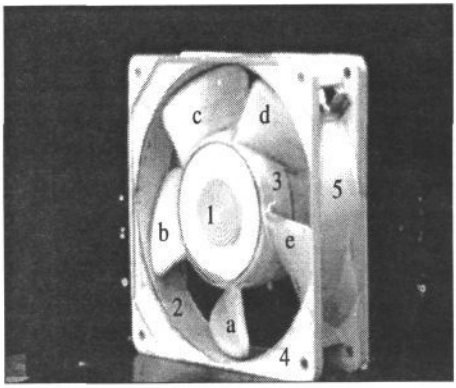

(a) Intensity picture of the scene.

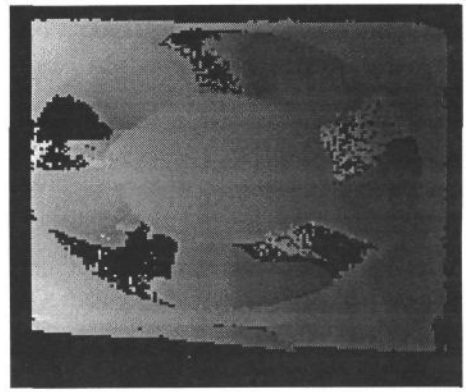

(b) Depth map (L), illumination angle 35 °.

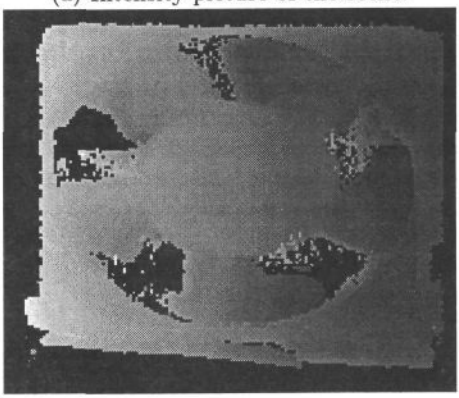

(c) Depth map (L), illumination angle 25 °.

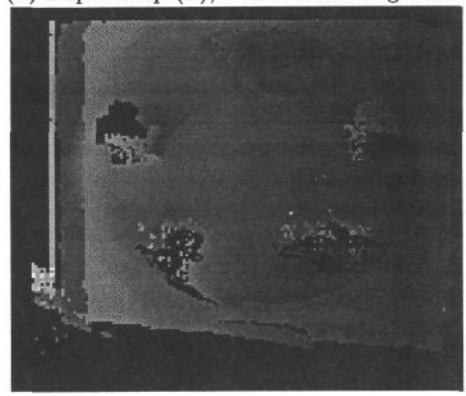

(d) Depth map (L), illumination angle 20 °.

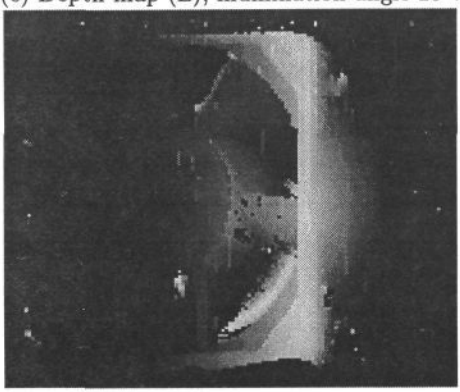

(e) Depth map (R), illumination angle 10 °

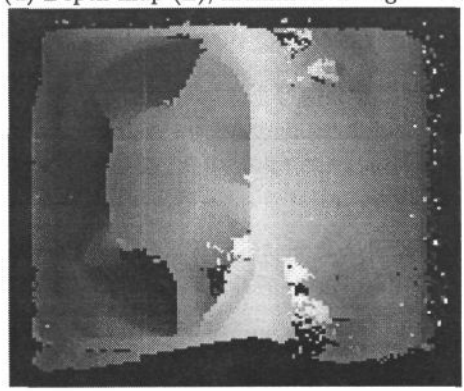

(f) Depth map (R), illumination angle 25 °.

Figure 7: Depth maps of a scene taken with five different geometries .

7 Acknowledgement

This research was funded by EPSRC GR/J07891, `Part Identification and Positioning by Sensor Fusion`. We would like to thank Frank Harrison and the technical staff in the Department of Physics for the manufacture of the planar elliptical mirrors. The work presented in this paper benefited greatly from discussions with Guanghua Zhang.

References

[1] Sabry F. El-Hakim and Nicolino J. Pizzi, *Multicamera vision-based approach to flexible feature measurement for inspection and reverse engineering*, Optical Engineering, September 1993, Vol 32 No. 9, pp2201-2215.

[2] Vassilios E. Theodoracatos, *Occlusion-free monocular three-dimensional vision system*, Optical Engineering, October 1994, Vol 33 No. 10, pp3476-3483.

[3] P. Besl, *Active, Optical Imaging Sensors*, Machine Vision and Applications, 1988, pp. 127 – 152.

[4] P. Saint-Marc, J.-L. Jezouin and G. Medioni, *A Versatile PC-Based Range Finding System*, IEEE Trans. Robot. Autom., vol. RA-7, no. 2, April 1991, pp. 250 –256.

[5] G.H. Zhang, J. Clark, A. M. Wallace, *Registered Depth and Intensity Data from an Integrated Vision Sensor*, Proc. SPIE 2348, Imaging and Illumination for Metrology and Inspection, Boston, November 1994.

[6] G. Zhang and A. M. Wallace, Physical modelling and combination of range and intensity edge data. CVGIP: *Image Understanding*, 58(2):191-220, 1993.

[7] G. Zhang and A. M. Wallace, Edge labelling by fusion of intensity and range data. In P. Mowforth, editor, *Proc. British Machine Vision Conf.*,pp. 412-415, 1991.

[8] C. Bradley and G. Vickers, Free-form surface reconstruction for machine vision rapid prototyping., *Optical Engineering* 32(9):2191, 1993

[9] D.K. Naidu and R. B. Fisher, A Comparitive Analysis of Algorithms for Determining the Peak Position of a Stripe to Sub-Pixel Accuracy. In P. Mowforth, editor, *Proc. British Machine Vision Conf.*,pp. 217-225, 1991.